AIChE

On the Quantification of the Controlling Regimes in Automotive Catalytic Converters

H. Santos
Mechanical Engineering Dept., School of Technology and Management, Polytechnic Institute of Leiria, Morro do Lena–Alto Vieiro Apt. 4163 2411-901 Leiria, Portugal

M. Costa
Mechanical Engineering Dept., Instituto Superior Técnico, Technical University of Lisbon, Avenida Rovisco Pais, 1049-001 Lisbon, Portugal

DOI 10.1002/aic.12252
Published online April 20, 2010 in Wiley Online Library (wileyonlinelibrary.com).

The conversion of pollutants in automotive catalytic converters is influenced by a number of physical and chemical processes that take place in the gaseous and solid phases as the exhaust gases flow through the converter. A detailed understanding of the complex processes involving flow dynamics, heat and mass transport and heterogeneous surface reactions is of crucial importance to improve the converter design. The main objective of the present study is to quantify the magnitudes of the external and internal mass transfer as well as chemical reaction limiting processes as a function of the converter operating temperature. To this end, experimental data, obtained for a three way catalyst (TWC) under real world operating conditions, are analyzed and compared against analytical expressions that allow for the quantification of the different limiting processes involved. The results demonstrate that (i) the external mass transfer resistance overlaps the reaction resistance only at moderate operating temperatures and not immediately above the ignition temperature as generally considered in the literature, (ii) the transport phenomena (external and internal mass transfer) represents 90% of the total resistance for temperatures higher than 792 K, (iii) the internal mass transfer in the porous washcoat presents a larger resistance than the external mass transfer from the bulk fluid to the washcoat wall even at high operating temperatures, and (iv) based on the quantification of the individual resistances as a function of the TWC operating temperature, it was demonstrated both the influence of the substrate cell density and of the effective diffusivity on the TWC conversions. © 2010 American Institute of Chemical Engineers *AIChE J,* 57: 218–226, 2011
Keywords: external mass transfer, internal mass transfer, chemical reaction, overall and individual resistances, controlling regimes

Introduction

Automotive catalytic converters are of crucial importance to control pollutant emissions from vehicles. Nowadays, the application of three way catalysts (TWC) to the exhaust gases of internal combustion engines allows a tremendous reduction of carbon monoxide (CO), partially burned or unburned hydrocarbons (HC) and oxides of nitrogen (NO_x).

Commonly, a TWC consists of monolithic structures of many parallel channels, coated with a porous material (washcoat). This porous material is usually alumina and has the objective of increasing the available surface area. The

Correspondence concerning this article should be addressed to M. Costa at mcosta@ist.utl.pt.

Table 1. Main Technical Attributes of the Catalyst Studied

Substrate Type	Square Cell Ceramic
Cell density (cells/cm^2)	62 (400 cpsi)
Substrate dimensions (mm)	Diameter = 127; L = 120
Catalyst volume (dm^3)	1.52
Uncoated geometric surface area (m^2/m^3)	2740
Coated geometric surface area (m^2/m^3)	2526
Uncoated wall thickness (mm)	0.1651 (6.5 mil)
Mean washcoat thickness (mm)	0.025
Open frontal area uncoated (%)	75.7
Open frontal area coated (%)	69.0
Cell hydraulic diameter uncoated (mm)	1.105
Washcoat material	CeO_2—Al_2O_3
Precious metal loading	7 Pd/1 Rh
Total mass of precious metal (g)	1.159

catalytic reactions take place on the noble metal particles distributed in the washcoat.

Design improvements of automotive catalytic converters require the broadening of the fundamental understanding of the various physical and chemical processes that occur in these devices. Overall, catalyst efficiency depends on the cold start behavior and conversions at normal operating temperatures (above ignition temperature). In the past, cold start emissions represented approximately 80% of the total emissions so that literature studies were focused mainly on enhancing the low temperature activity (e.g., Skoglundh and Fridell[1]).

During cold start and before ignition, the TWC works as a heat exchanger. This means that the mass of the converter is heated up by the exhaust gases. The heat transfer between the exhaust gases and the channel surface is determined by the geometric surface area, the cell density (hydraulic diameter), the velocity of the gas flow and the substrate thermal properties, such as the specific heat capacity and the thermal conductivity. The influence of these parameters on the cold start behavior of TWCs is well documented in the literature (e.g., Pfalzgraf et al.[2]).

After the substrate heat up, different factors influence the TWC conversions, all of them depending largely on the operating temperature. The conversions of the exhaust gaseous pollutants in a TWC channel are controlled by three individual processes in series, namely, external mass transfer (between the bulk gas and the washcoat surface), internal mass transfer (pore diffusion) and chemical reactions (Hayes and Kolaczkowski[3]).

Design and optimization of a catalytic converter is challenging due to the complex interaction between transport phenomena and chemical reactions. Under these circumstances, quantification of the influence of each individual process on the conversions is of crucial importance to provide guidelines for further catalytic converter improvements.

In general, the studies available in the literature demonstrate that the ignition in a TWC is controlled mainly by chemical reaction effects (e.g., Kašpar et al.[4]), being the conversions dependent mainly on the external mass transfer process at normal operating temperatures (e.g., Umehara et al.[5], Brück et al.,[6] and Ramanathan et al.[7]). However, in a recent article (Santos and Costa[8]), we have found that even at high temperatures and mass flow rates (MAFs), purely external mass transfer controlled regime is hard to obtain under realistic operating conditions.

In spite of the large number of studies available in the literature on automotive catalytic converters, the simultaneously quantification of the three individual resistances (external, internal, and reaction) as a function of the operating temperature in the converter remains an open issue. The main goal of this article is to provide such quantification.

This article presents data from a number of experiments that were carried out at normal operating temperatures. The TWC was tested directly in the vehicle exhaust system to reproduce real word operating conditions. Flow, temperature, and chemical species conversion data was used to evaluate the overall mass transfer resistance to the conversions in the TWC. To quantify each individual resistance, the analytical expressions recently derived by Joshi et al.[9] were used to fit the present experimental data. Subsequently, based on the present quantification for controlling regimes, it was evaluated that both the influence of the substrate cell density and of the effective diffusivity on the TWC conversions.

Test section, Instrumentation, and Procedures

The measurements reported here were carried out on a vehicle equipped with a 2.8 l spark ignition engine. The vehicle was tested on a chassis dynamometer under steady state for a variety of operating conditions to study the TWC conversions. One commercial TWC was studied, being their characteristics presented in Table 1. To perform the experiments, the TWC was in turn placed in the so-called underfloor position replacing the original TWC installed on the vehicle.

Figure 1 shows a schematic of the experimental setup. The data was monitored continuously by two data acquisition boards. The data provided by the engine sensors was also monitored using an engine diagnostic scanner connected to a diagnostic link (On Board Diagnostic port), located within the vehicle below the dashboard. The data obtained include inlet MAF, manifold absolute pressure, engine operating temperatures, engine speed, signals from the lambda sensors, exhaust gas species concentrations and temperatures taken both upstream and downstream of the TWC, as well as temperatures in various locations within the substrate of the TWC.

In the present work, the engine inlet mass air flow and the lambda signals were acquired from the vehicle sensors (hot film MAF anemometer and engine lambda sensor, respectively) to evaluate the exhaust MAF.

Figure 2 presents a photograph of the exhaust after-treatment system showing the TWC, the exhaust gas sampling probes, the lambda sensors, and the thermocouples. Exhaust gas oxygen sensors, commonly denominated as lambda sensors, are essential for TWC monitoring and control. In the present study, the engine was controlled by the original engine control unit. However, to verify the mixture stoichiometry both upstream and downstream of the TWC, two additional lambda sensors have been installed, as shown in Figures 1 and 2.

Exhaust gases were sampled from the exhaust pipe both upstream and downstream of the TWC with the aid of stainless steel sampling probes, as shown in Figure 2. Figure 3

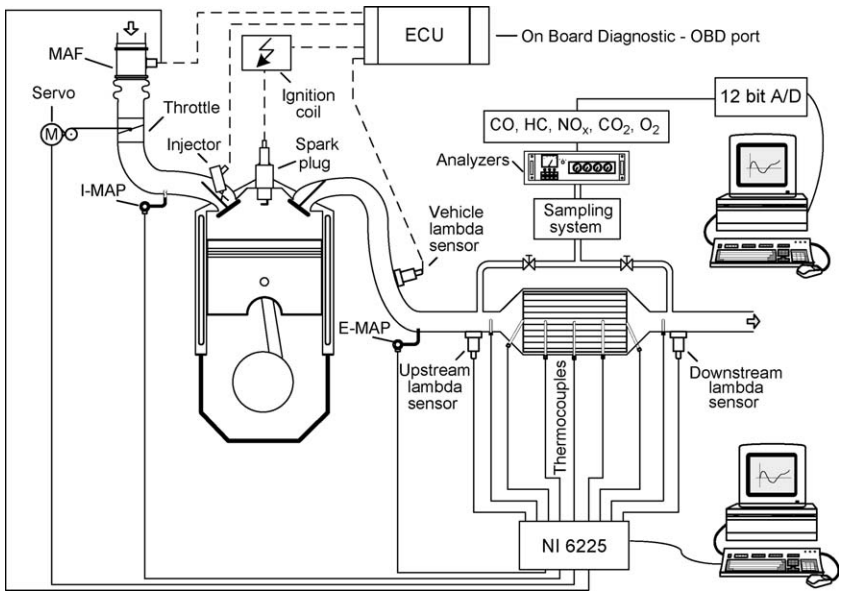

Figure 1. Schematic of the experimental setup.

shows a schematic of the exhaust gas sampling system. The analytical instrumentation includes a magnetic pressure analyzer for O_2 measurements, non dispersive infrared gas analyzers for CO_2 and CO measurements, a flame ionization detector for HC measurements and a chemiluminescent analyzer for NO_x measurements. Zero and span calibrations with standard mixtures were performed before and after each measurement session. The maximum drift in the calibration was within $\pm 2\%$ of the full scale.

Conversions at Normal Operating Temperatures

Table 2 summarizes the test conditions for which the present study was performed. For each engine speed (2000, 3000, and 4000 rpm) tests were made for six different loads [break mean effective pressure (BMEP)]. The 18 test conditions led to exhaust MAFs ranging from 43.5 to 266.4 kg/h. Note that a medium class vehicle tested via the Federal Test Procedure (FTP) cycle operates with exhaust gas MAFs between 0 and 140 kg/h. In the present work, steady-state test conditions were chosen to take into account not only a medium class vehicle tested on the FTP cycle but also the high speed driving, which is not included in any emission test.

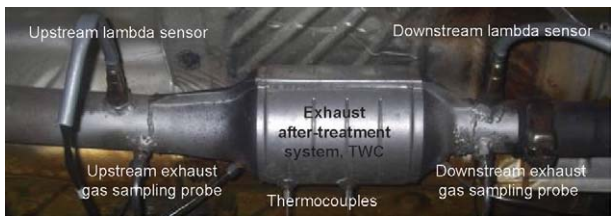

Figure 2. Photograph of the exhaust after treatment system showing the TWC, the exhaust gas sampling probes, the lambda sensors and the thermocouples.

[Color figure can be viewed in the online issue, which is available at wileyonlinelibrary.com.]

Figure 4 shows the measured CO, HC, and NO_x conversions as a function of the operating temperature in the TWC. It should be noted that the conversions presented in Figure 4 are based on real engine-out emissions (see Table 2). It is seen that the conversions are higher for NO_x followed by the CO and HC conversions, respectively. Figure 4 reveals that the conversions decrease for high operating temperatures, regardless of the chemical species. Furthermore, HC conversions appear to be the most sensitive to temperature. This means that the low reaction times (high temperatures) are not sufficient to compensate the low residence times (high exhaust MAF, see Table 2) and, consequently, the conversions decreases as the temperature increases.

It has been shown in various studies (e.g., Pfalzgraf et al.[2] and Ramanathan et al.[7]) that cold start emissions can be significantly reduced through the installation of the catalytic converter closer to the engine, which also leads to high normal operating temperatures. Consequently, to achieve future European emission standards (e.g., EURO VI), in addition to the cold start, the conversions at normal operating temperatures will also become increasingly important.

The data in Figure 4 indicate that the TWC conversions can be further improved towards the 100% limit. Therefore, the study of the limiting factors as a function of the operating temperature in the TWC is of primary importance for the identification of the most critical design parameters that are limiting the conversions.

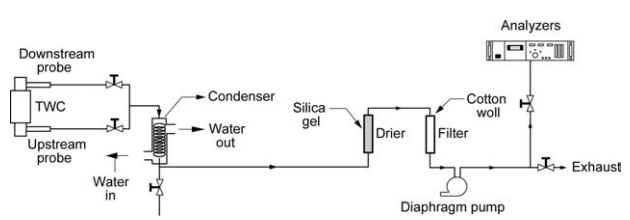

Figure 3. Schematic of the exhaust gas sampling system.

Table 2. Test Conditions

Vehicle		Three Way Catalyst				
Engine Speed (rpm)	BMEP (bar)	Operating Temperature (K)	Exhaust Mass Flow Rate (kg/h)	Upstream TWC, CO (%)	Upstream TWC, HC (ppm)	Upstream TWC, NO_x (ppm)
2000	0.00	638	43.5	0.62	231	241
	0.90	695	63.5	0.60	484	1180
	1.66	741	80.0	0.59	517	1542
	2.28	765	91.2	0.62	503	1570
	2.65	792	100.6	0.62	480	1646
	2.91	802	101.2	0.62	537	2089
3000	0.00	730	68.7	0.65	223	512
	0.97	841	101.9	0.91	333	1149
	1.92	892	126.9	0.91	324	1547
	2.91	926	150.4	0.96	338	1963
	3.68	962	174.6	0.97	337	2333
	4.49	1002	197.9	0.96	220	2458
4000	0.00	809	96.3	0.69	191	1371
	1.01	926	143.7	0.70	270	2734
	2.00	971	170.6	0.74	249	3169
	2.98	1004	206.8	0.83	242	3307
	4.07	1038	238.5	0.81	230	3279
	5.25	1074	266.4	0.79	147	3134

Quantification of the Mass Transfer and Reaction Resistances

This section quantifies the overall mass transfer resistance (R_t) and the individual resistances. To this end, the definition of overall mass transfer resistance provided by Joshi et al.[9] was used. Following these authors, the overall mass transfer resistance comprises three resistances in series: external mass transfer (R_{ext}), internal mass transfer (R_{int}) and reaction (R_r). The individual resistances are expressed as follows:

$$R_{ext,i} = \frac{1}{k_{ext,i}}; \quad R_{int,i} = \frac{1}{k_{int,i}}; \quad R_{r,i} = \frac{1}{k_{V,i} \cdot \delta_C}. \tag{1}$$

The overall resistance is simply the sum of the individual resistances:

$$R_{t,i} = \frac{1}{k_{ov,i}} = R_{ext,i} + R_{int,i} + R_{r,i}. \tag{2}$$

Comparing Eqs. 1 and 2 the expression for the quantification of the resistances can be written as:

$$\frac{1}{k_{ov,i}} = \frac{1}{k_{ext,i}} + \frac{1}{k_{int,i}} + \frac{1}{k_{V,i} \cdot \delta_C} \tag{3}$$

It should be noted that $k_{ov,i}$ is the overall mass transfer coefficient measured experimentally that includes the effects of the external and internal mass transfer and that of the reaction in the washcoat. Because it includes reaction effects, Joshi et al.[9] refer to $k_{ov,i}$ as an apparent mass transfer coefficient, which was evaluated as follows:

$$k_{ov,i} = -\frac{\ln(1 - X_i)}{\frac{A}{V} t_c} \tag{4}$$

From Eq. 4 it can be concluded that $k_{ov,i}$ depends on the TWC mass transfer area per unit of catalyst volume (A/V), on the convection (residence) time (t_c) and on the conversion data (X_i). The conversion data incorporates a combination of reaction and mass transfer limitations.

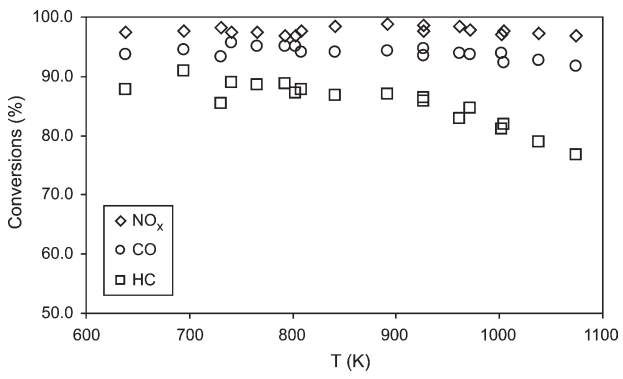

Figure 4. Measured CO, HC and NO_x conversions as a function of the operating temperature in the TWC.

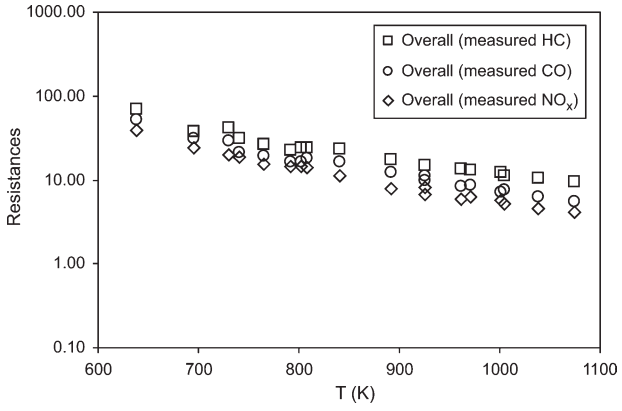

Figure 5. Overall (measured) resistance for CO, HC, and NO_x conversions as a function of the operating temperature in the TWC.

Based on the measured data, $R_{t,i}$ was evaluated for each operating condition for the three chemical species under study. Figure 5 shows the overall (measured) resistance for CO, HC, and NO_x conversions as a function of the operating temperature in the TWC. The figure indicates that for the three chemical gas species studied the overall resistance decreases with the temperature. Note that Figure 4 reveals that in general the conversions tend to decrease with the temperature, but, on the other hand, Table 2 indicates that the exhaust MAF strongly increases with the temperature, while the residence time decreases. However, the residence time decreases much more with the temperature than the TWC conversions. As a result of the two combined effects the magnitude of the overall resistance decreases as the temperature increases for the present practical operating conditions. Returning to Figure 5, it is also seen that the magnitude of the overall resistance is higher for HC, followed by that of the CO and then by that of the NO_x.

As CO is present in the vehicle exhaust in higher concentrations than HC and NO_x (see Table 2), the CO may be considered as a representative gas species in the TWC. Hence, CO conversion is representative of the behavior of the whole system and, for this reason, we concentrate below solely on the analysis for CO. For the quantification of the individual resistances, external and internal mass transfer coefficients were evaluated through the respective external and internal Sherwood numbers:

$$\mathrm{Sh}_{\mathrm{ext}} = \frac{k_{\mathrm{ext}} d}{D_{\mathrm{m}}}, \tag{5}$$

$$\mathrm{Sh}_{\mathrm{int}} = \frac{k_{\mathrm{int}} \delta_{\mathrm{C}}}{D_{\mathrm{eff}}}. \tag{6}$$

External Sherwood numbers cannot be measured experimentally and, thus, need to be estimated using appropriate correlations. Correlations for estimating the external Sherwood in ducts of various shapes in which the flow is laminar have been presented and discussed by Hawthorn,[10] Tronconi and Forzatti,[11] Gupta and Balakotaiah,[12] Ramanathan et al.,[7] and Bhattacharya et al.,[13] among others. In the present study, the external Sherwood was evaluated using the correlation proposed by Hawthorn,[10] which has been based on the analytical solution presented by Kays and London.[14]

To simplify the problem of diffusion and reaction in the washcoat, Balakotaiah[15] developed the internal Sherwood number concept. Subsequently, Joshi et al.[16,17] applied this concept to the modeling of diffusion and reaction in catalytic monoliths. Appendix A presents the method used in the present study to evaluate the internal Sherwood number.

In addition to the internal Sherwood number, the accurate knowledge of the effective diffusion in the washcoat (D_{eff}) is crucial for the evaluation of the internal mass transfer coefficient (see Eq. 6). The typical CeO_2—Al_2O_3 washcoat, widely used in commercial TWCs, has a bi-modal pore size distribution composed mainly by small mesopores of about 10 nm and by macropores (pore diameter in the range of 100–500 nm and volume fraction around 20%) (Zhang et al.[18] and Starý et al.[19]). Mesopores are prevalent in the washcoat and therefore the Knudsen diffusion dominates. As a result, the dependence of the temperature and gas species, as typified

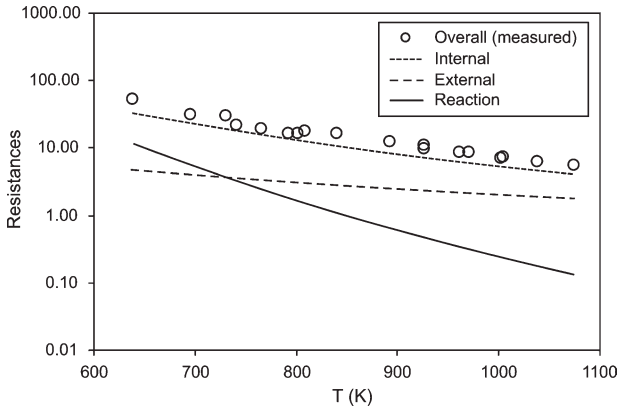

Figure 6. Overall (measured) resistance and individual resistances (external, internal and reaction) as a function of the operating temperature in the TWC.

by the molecular weight, of the effective diffusivity can be expressed as:

$$D_{\mathrm{eff,i}}(T) = D_{\mathrm{eff,ref}} \sqrt{\frac{T_{\mathrm{W}}}{T_{\mathrm{ref}}}} \sqrt{\frac{M_{\mathrm{ref}}}{M_{\mathrm{i}}}} \tag{7}$$

where the chosen reference chemical species is the CO and T_{ref} is equal to 296 K. In the present study, $D_{\mathrm{eff,ref}}$ was taken equal to 1.13×10^{-7} m^2 s^{-1}, based on recent experimental data (Starý et al.[19]).

The evaluation of the reaction resistance was performed using the volumetric rate constant, k_{v}, which was modeled through an Arrhenius rate expression as in most similar works. Several simulations were carried out to establish the appropriate reaction parameters (pre-exponential factor and activation energy). After each simulation the predicted conversion data was compared to the experimental data. The least squares error was computed as the sum of the squares of the computed errors for the 18 steady state test conditions. The sum of the squares was minimized for the best fit generating values for the pre-exponential factor and activation energy. This procedure yielded the following CO volumetric rate constant k_{v}:

$$k_{\mathrm{v}} = 2.06 \times 10^8 \exp\left(-\frac{59,600}{R \cdot T_{\mathrm{W}}}\right) \tag{8}$$

The individual resistances were then calculated using Eq. 1. Figure 6 shows the overall (measured) resistance and the individual resistances (external, internal, and reaction) as a function of the operating temperature in the TWC. The figure demonstrates that each resistance is a monotonic decreasing function of temperature, though the external mass transfer resistance is nearly independent of temperature. Figure 6 also reveals that for the temperature interval considered here the magnitude of the internal mass transfer resistance is dominant. Figure 6 also demonstrates that as the temperature increases the reaction resistance significantly decreases. The reaction rate increases exponentially following the Arrhenius law. As a result, at sufficiently high temperature the

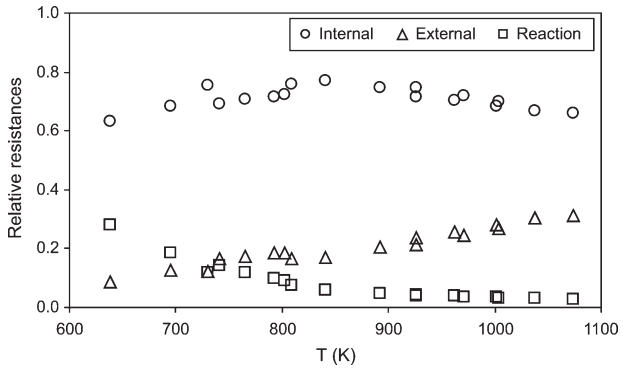

Figure 7. Relative magnitude of each individual resistance (external, internal and reaction) as a function of the operating temperature in the TWC.

characteristic reaction time approaches zero and the magnitude of the reaction resistance is negligible.

Subsequently, the relative magnitude of each individual resistance was evaluated. To this end, the individual relative resistances were evaluated as a fraction of the total resistance. Figure 7 shows the relative magnitude of each individual resistance (external, internal, and reaction) as a function of the operating temperature in the TWC. The figure reveals that the relative reaction resistance is a monotonic decreasing function of temperature, being the relative external mass transfer resistance a monotonic increasing function of temperature. However, it is important to observe that the relative internal mass transfer resistance is not a monotonic function of the temperature.

Figure 7 shows that in the temperature interval considered ($630\ \text{K} < T < 1074\ \text{K}$), the relative magnitude of the internal mass transfer resistance is the largest, varying between 0.63 and 0.77, with a maximum located at intermediate temperatures ($T \approx 840$ K). Figure 7 also demonstrates that at temperatures lower than 730 K the reaction resistance overlaps the external mass transfer resistance. This is a quite surprising result because, above ignition temperatures, it is generally considered that the external mass transfer resistance overlaps the reaction resistance (e.g., Brück et al.[6]). This study demonstrates that this is far from true, indicating that the reaction resistance can play an important role for a range of moderate operating temperatures above ignition. As a consequence, the assumption that the external mass transfer is the rate-limiting process can lead to erroneous conclusions about the design parameters that control the conversions above ignition temperatures.

In the work referred earlier, Joshi et al.[9] defined three characteristic regimes that can prevail in a monolith depending upon the design and operating parameters as follows:

$R_r \geq 0.9R_t$ for the kinetic regime,

$R_{ext} \geq 0.9R_t$ for the external mass transfer controlled regime, and

$R_{int} \geq 0.9R_t$ for the internal mass transfer controlled regime.

In this study, these practical criteria have been used to analyze the experimental data. Figure 7 shows that, under the present operating conditions, the TWC does not operate in none of the regimes defined by Joshi et al.[9] so that it is impossible to identify the controlling regime based on the criteria proposed by these authors. In light of this, we have extended the criteria proposed by Joshi et al.[9] to take into account the mixed regimes observed under the present operating conditions as follows:

$$R_r + R_{int} \geq 0.9R_t, \tag{9}$$

for a kinetic and internal mass transfer mixed controlled regime and

$$R_{int} + R_{ext} \geq 0.9R_t, \tag{10}$$

for an internal and external mass transfer mixed controlled regime. If none of the two conditions apply, a total mixed regime with kinetic, internal and external mass transfer controlling will be established.

Based on Eqs. 9 and 10, Figure 8 shows the controlling regimes as a function of the operating temperature in the TWC. The figure illustrates the applicability of the criteria proposed in the present study to classify the different mixed regimes that can prevail in a TWC operating under real world operating conditions. Figure 8 demonstrates that the kinetic and internal mass transfer mixed controlled regime prevails at temperatures lower than 638 K. The total mixed regime (kinetic, internal and external mass transfer controlling) prevails in the temperature interval from 638 to 792 K and, finally, the internal and external mass transfer mixed controlled regime prevails at temperatures higher than 792 K.

The present quantification of the controlling regimes was here performed for a TWC, which is usually operated under stoichiometric conditions. Other automotive catalytic converters [e.g., diesel oxidation catalyst (DOC), lean NO_x trap (LNT), and selective catalytic reduction (SCR)] usually operate under lean conditions. In general, automotive catalytic converters operate with relatively low reactants concentration as compared with other converters (like catalytic combustors). In addition, they use similar structures (channel like). As a result, it can be expected that the conclusions drawn from the present study for the external mass transfer will apply to other automotive catalytic converters. Nevertheless, DOC, LNT, and SCR generally operate at low temperatures as compared with TWC so that further investigation is required to evaluate the relative resistances as a function of the operating temperature in such converters.

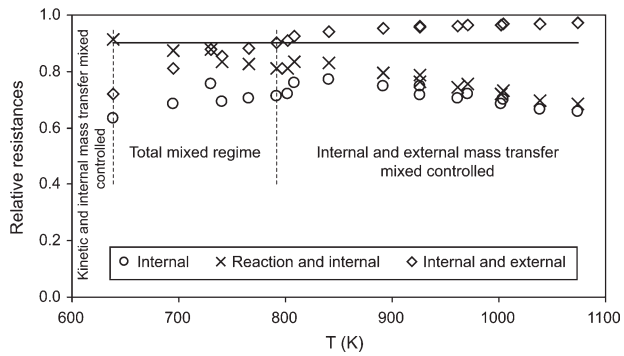

Figure 8. Controlling regimes as a function of the operating temperature in the TWC.

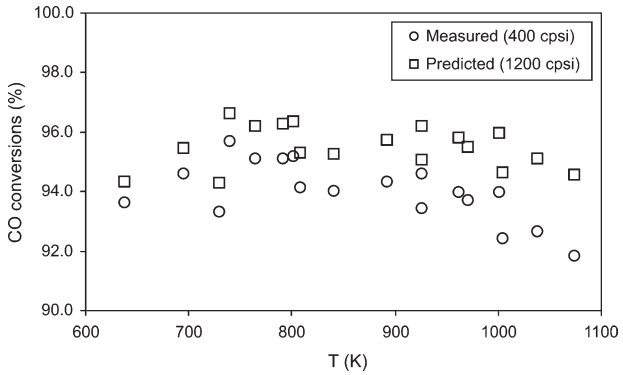

Figure 9. Measured CO conversions for the catalyst studied (see Table 1) and predicted CO conversions for a catalyst with 1200 cpsi as a function of the operating temperature in the TWC.

Influence of the Design Parameters on the TWC Conversions

In the previous section, the controlling regimes were identified as a function of the operating temperature in the TWC. The increase of the TWC conversions at acceptable costs demands design improvements without increasing the precious metal loading (PML). It is important, therefore, to study the design parameters that influence both the external and internal mass transfer resistances at normal operating temperatures.

Influence of the substrate cells density

As discussed in the introduction, a number of previous studies had considered that above ignition the external mass transfer is the rate limiting process. In the last few years, the improvements in the TWC conversions at normal operating temperatures were achieved mainly through advances on the external mass transfer of the monolith converters. To accomplish this, for example, both metallic and ceramic substrates with high cell densities and thin foils have been introduced (Avila et al.[20]).

An increase in cell density means an enlargement of the geometrical surface area, a reduction in hydraulic diameter and high external mass transfer coefficients, but with the disadvantage of high back pressure due to the reduction of the open frontal area. However, this disadvantage can be overcome by reducing the substrate wall thickness (Umehara et al.[5]). As an example, for the same open frontal area increasing the cell density from 400 cpsi to 800 cpsi and to 1200 cpsi increases the external mass transfer coefficient by 44% and 80%, respectively, without pressure loss penalties.

Figure 9 shows the measured CO conversions for the catalyst studied (see Table 1) and the predicted CO conversions for a catalyst with 1200 cpsi as a function of the operating temperature in the TWC. In the operating temperature interval studied here the measured CO conversions (catalyst studied, 400 cpsi) vary from 91.8% to 95.7% while the predicted CO conversions for a catalyst with a 1200 cpsi substrate vary between 94.3% and 96.6%. The predicted results indicate that high cells densities lead to high conversions. This positive influence becomes more significant as the operating temperature in the TWC increases, which indicates that the use of a substrate with high cell density is particularly important when the TWC is installed in the so-called close coupled position.

High cell densities result in lower external mass transfer resistance and, therefore, in improved TWC efficiencies under normal operating temperatures, as indicated in Figure 9. This design improvement was widely implemented in the last years to fulfill the emissions legislation.

Influence of the effective diffusivity

In the present work, it was found that the internal mass transfer resistance is the most important resistance over the range of normal operating temperatures considered here. The internal mass transfer resistance can be reduced by favoring the accessibility of the reactants towards the active sites located within the washcoat structure. In this respect, an enormous progress has recently been made in the field of ordered porous structured materials. Studies concerning the synthesis of materials with controlled micro-meso-macro–pore structures and metal oxides such as alumina, silica, titania or zirconia are now available in the literature (see, e.g., Suárez et al.[21] and Yuan and Su[22]).

The recent results of Suárez et al.[21] and Yuan and Su[22] demonstrate that enhanced washcoat structures allowed for a substantial increase in macropores volume. As a consequence, the effective diffusivity may increase considerably. To study this effect in the TWC conversions, the reference effective diffusivity in Eq. 7 was increased by a factor of 2, with all remaining washcoat properties being kept constant.

Figure 10 shows the measured CO conversions for the catalyst studied (see Table 1) and the predicted CO conversions for a catalyst with double effective diffusivity as a function of the operating temperature in the TWC. The figure demonstrates that the use of a washcoat structure with high effective diffusivity contributes significantly to augment the TWC conversions; specifically, the predicted conversions are in the range 96.6–99.3% as compared to 91.8–95.7% for the catalyst studied.

A comparison between Figures 9 and 10 demonstrates that particularly at moderate operating temperatures (<1000 K) to double the effective diffusivity is much more useful than to increase the substrate cells density from 400 cpsi to 1200 cpsi. Nevertheless, at high operating temperatures (>1000 K), the increase in substrate cell density for 1200 cpsi allows

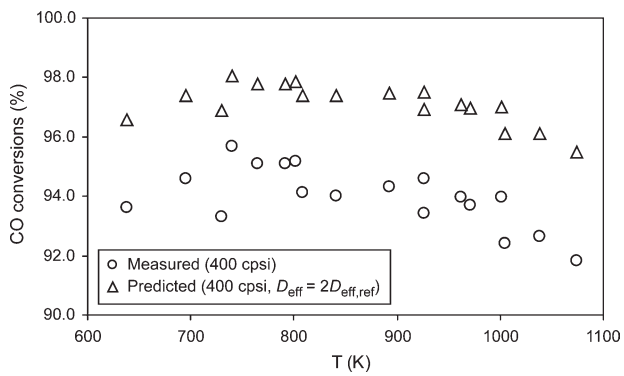

Figure 10. Measured CO conversions for the catalyst studied (see Table 1) and predicted CO conversions for a catalyst with double effective diffusivity as a function of the operating temperature in the TWC.

to attain TWC conversions closer to those for 400 cpsi with double effective diffusivity.

Simultaneously influence of the cell density and effective diffusivity

Future emissions legislation will require increasingly efficient TWC so that an important goal is to increase the conversions to around 100%. The ultimate approach will be to use a TWC with both high cell density and effective diffusivity. Figure 11 shows the measured CO conversions for the catalyst studied (see Table 1) and the predicted CO conversions for a catalyst with 1200 cpsi and double effective diffusivity as a function of the operating temperature in the TWC. As expected, Figure 11 reveals that the conversions for the 1200 cpsi with double effective diffusivity are higher than those achieved with the previous approaches (see Figures 9 and 10). Figure 11 demonstrates that the conversions are always above 97.1% for the wide range of temperatures studied, as compared to 91.8% for the catalyst experimentally studied here.

A comparison between Figures 9, 10, and 11 allows observing that a TWC with both high cell density and effective diffusivity yields uniform and high conversions regardless of the operating temperature. As a result, it can be concluded that both internal and external mass transfer resistances need to decrease to attain high conversion for a wide range of operating temperatures.

As a final remark, it should be pointed out that the present study demonstrates that under normal operating temperatures the TWC conversions could be significantly improved without changing the PML. The external mass transfer resistance cannot be reduced by increasing the PML but, on the other hand, both the internal mass transfer and reaction resistances decrease as the PML increases. Note, however, that an increase in PML will not only promote high TWC conversions, but also will contribute to high production costs.

Conclusions

To the best of our knowledge, the current study presents the first attempt to quantify the external, internal and reaction resistances in automotive catalytic converters. From the analysis of the results the following conclusions can be drawn:

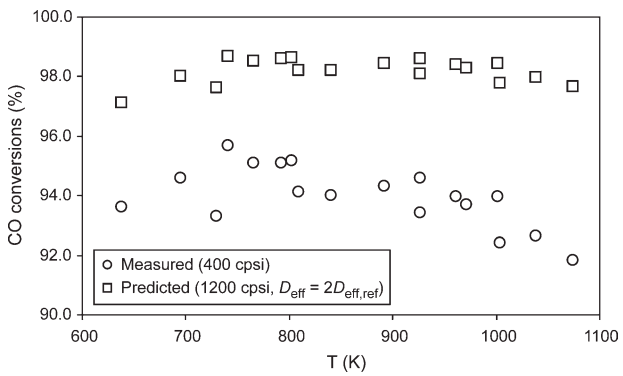

Figure 11. Measured CO conversions for the catalyst studied (see Table 1) and predicted CO conversions for a catalyst with 1200 cpsi and double effective diffusivity as a function of the operating temperature in the TWC.

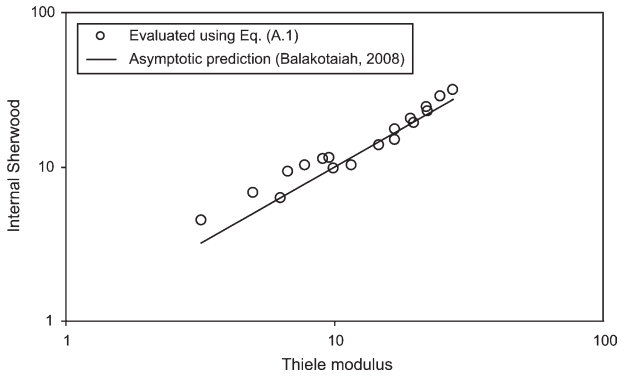

Figure A1. Internal Sherwood number evaluated using Eq. A1 and using the asymptotic prediction ($Sh_{int} = \phi$, Balakotaiah[15]) as a function of the washcoat Thiele modulus.

- the external mass transfer resistance overlaps the reaction resistance only at moderate operating temperatures and not immediately above the ignition temperature as generally considered in the literature,
- the transport phenomena (external and internal mass transfer) represents 90% of the total resistance for temperatures higher than 792 K,
- the internal mass transfer in the porous washcoat presents a larger resistance than the external mass transfer from the bulk fluid to the washcoat wall even at high operating temperatures, and
- based on the quantification of the individual resistances as a function of the TWC operating temperature, it was demonstrated both the influence of the substrate cell density and of the effective diffusivity on the TWC conversions, namely it was found that the increase in substrate cell density and in the effective diffusivity permits to increase the conversions, while it was also verified that their benefits depends on the operating temperature.

Acknowledgment

H. Santos acknowledges the Fundação para a Ciência e a Tecnologia for the provision of the scholarship SFRH/BD/32851/2006.

Notation

d = hydraulic diameter of monolith cell channel, m
D_{eff} = effective diffusion in the washcoat, m^2/s
$D_{eff,ref}$ = effective diffusion of the reference species, m^2/s
D_m = molecular diffusion in the gas phase, m^2/s
k_{ext} = external mass transfer coefficient, m/s
k_{int} = internal mass transfer coefficient, m/s
k_{ov} = overall mass transfer coefficient, m/s
k_V = reaction rate constant per volume of washcoat, 1/s
M = molecular weight of the chemical species, kg/mol
M_{ref} = molecular weight of the reference species, kg/mol
R = universal gas constant, J/mol/K
R_t = total mass transfer resistance
R_{ext} = external mass transfer resistance
R_{int} = internal mass transfer resistance
R_t = reaction resistance
Sh_{ext} = external Sherwood number
Sh_{int} = internal Sherwood number
Sh_{ov} = overall Sherwood number
T_{ref} = reference temperature, K
T_W = solid wall temperature, K
t_c = convection (residence) time, s

Greek letters

δ_C = effective washcoat thickness, m
μ = ratio of reactant diffusivities in the gas phase and in the washcoat
λ = ratio of diffusion lengths, $\lambda = \frac{4\delta_c}{d}$
ϕ = washcoat Thiele modulus

Literature Cited

1. Skoglundh M, Fridell M. Strategies for enhancing low-temperature activity. *Top Catal*. 2004;28:79–87.
2. Pfalzgraf B, Rieger M, Ottowitz G. Close coupled catalytic converters for compliance with LEV/ULEV and EG III legislation—influence of support material, cell density and mass on emission results. SAE Technical Paper series. Society of Automotive Engineers: Warrendale, Pennsylvania, USA. Paper no. 960261, 1996.
3. Hayes RE, Kolaczkowski ST. Mass and heat transfer effects in catalytic monolith reactors. *Chem Eng Sci*. 1994;49:3587–3599.
4. Kašpar J, Fornasiero P, Hickey N. Automotive catalytic converters: current status and some perspectives. *Catal Today*. 2003;77:419–449.
5. Umehara K, Makino M, Brayer M, Becker ER, Watson R. Prediction of catalytic performance for ultra thin wall and high cell density substrates. SAE Technical Paper series. Paper no. 2000–01-0494, 2000.
6. Brück R, Kaiser F, Konieczny R, Webb CC, Anderson A. Study of modern application strategies for catalytic aftertreatment demonstrated on a production V6 engine. SAE Technical Paper series. Paper no. 2001–01-0925, 2001
7. Ramanathan K, Balakotaiah V, West DH. Light-off criterion and transient analysis of catalytic monoliths. *Chem Eng Sci*. 2003;58:1381–1405.
8. Santos H, Costa M. The relative importance of external and internal transport phenomena in three way catalysts. *Int J Heat Mass Transfer*. 2008;51:1409–1422.
9. Joshi SY, Harold MP, Balakotaiah V. Overall mass transfer coefficients and controlling regimes in catalytic monoliths. *Chem Eng Sci*. 2010;65:1729–1747.
10. Hawthorn RD. Afterburner catalysts-effects of heat and mass transfer between gas and catalyst surface. *AIChE J*. 1974;21:849–853.
11. Tronconi E, Forzatti P. Adequacy of lumped parameter models for SCR reactors with monolithic structures. *AIChE J*. 1992;38:201–210.
12. Gupta N, Balakotaiah V. Heat and mass transfer coefficients in catalytic monoliths. *Chem Eng Sci*. 2001;6:4771–4786.
13. Bhattacharya M, Harold MP, Balakotaiah V. Mass-transfer coefficients in washcoated monoliths. *AIChE J*. 2004;50:2939–2955.
14. Kays WM, London AL. *Compact Heat Exchangers*, McGraw-Hill, New York, 1964.
15. Balakotaiah V. On the relationship between Aris and Sherwood numbers and friction and effectiveness factors. *Chem Eng Sci*. 2008;63:5802–5812.
16. Joshi SY, Harold MP, Balakotaiah V. Low-dimensional models for real time simulations of catalytic monoliths. *AIChE J*. 2009;55:1771–1783.
17. Joshi SY. Harold MP, Balakotaiah V. On the use of internal mass transfer coefficients in modeling of diffusion and reaction in catalytic monoliths. *Chem Eng Sci*. 2009;64:4976–4991.
18. Zhang F, Hayes RE, Kolaczkowski ST. A new technique to measure the effective diffusivity in the washcoat of a monolith reactor. *Chem Eng Res Des*. 2004;82:481–489.
19. Starý T, Šolcová O, Schneider P, Marek M. Effective diffusivities and pore-transport characteristics of washcoated ceramic monolith for automotive catalytic converter. *Chem Eng Sci*. 2006;61:5934–5943.
20. Avila P, Montes M, Miró EE. Monolithic reactors for environmental applications: a review on preparation technologies. *Chem Eng Sci*. 2005;109:11–36.
21. Suárez S, Yates M, Avila P, Blanco J. New TiO_2 monolith supports based on the improvement of the porosity. *Catal Today*. 2005;105:499–506.
22. Yuan ZY, Su BL. Insights into hierarchically meso-macroporous structured materials. *J Mater Chem*. 2006;16:663–677.

Appendix A: Evaluation of the Internal Sherwood Number

Balakotaiah[15] developed the concept and proposed a general approximation for the internal Sherwood number (Sh_{int}). The approximation has two asymptotes: slow reaction (given by $Sh_{int} = Sh_{int,\infty}$ for $\phi \ll 1$) and fast reaction (given by $Sh_{int} = \phi$ for $\phi \gg 1$). In a subsequent study, Joshi et al.[18] determined numerically the dependence of the internal Sherwood number on the washcoat and channel geometric shapes, reaction kinetics, catalyst loading and activity profile. The authors concluded that in catalytic monoliths, Sh_{int} jumps from slow reaction asymptote (before ignition) to fast reaction asymptote (after ignition) and the transition region is practically negligible. These authors concluded that the general approximation proposed by Balakotaiah[15] can be used for any washcoat-channel shape and any kinetics with sufficient accuracy.

The present data were gathered for TWC temperatures above ignition so that it was expectable that the fast reaction asymptotic ($Sh_{int} = \phi$) provided a good approximation for the internal Sherwood number (Sh_{int}). To verify the adequacy of this approximation and based on the equation for the overall Sherwood number (Sh_{ov}), derived by Joshi et al.[17], we derive the following expression for Sh_{int}:

$$Sh_{int} = \frac{\mu\lambda}{4\left[\frac{1}{Sh_{ov}} - \left(\frac{1}{Sh_{ext}} + \frac{\mu\lambda}{4\phi^2}\right)\right]}. \quad \text{(A1)}$$

Equation A1 indicates that the Sh_{int} can be evaluated knowing the measured overall Sherwood number, the external Sherwood number, the channel and washcoat properties and the Thiele modulus that depends on both washcoat properties and reaction kinetics. The method used for the evaluation of the Thiele modulus is presented and discussed in Santos and Costa[8].

Given the definitions above, the internal Sherwood number was evaluated using Eq. A1. Figure A1 shows the internal Sherwood number evaluated using Eq. A1 and using the asymptotic prediction ($Sh_{int} = \phi$, Balakotaiah[15]) as a function of the washcoat Thiele modulus. Note that in the present study the Thiele modulus is in the range 3.2–27.5 and the asymptotic prediction is fully valid only when $\phi \gg 1$. Figure A1 shows that, in general, the values obtained using Eq. A1 are in good agreement with the asymptotic prediction ($Sh_{int} = \phi$) for the Thiele modulus range under study. Figure A1 also demonstrates that as the Thiele modulus increases the Sh_{int} evaluated through Eq. A1 converges progressively to the asymptotic prediction ($Sh_{int} = \phi$).

Manuscript received Dec. 22, 2009, and revision received Feb. 11, 2010.